





Entanglement purification on quantum networks

Michelle Victora ¹, Spyros Tserkis ², Stefan Krastanov,^{2,3} Alexander Sanchez de la Cerda,²
Steven Willis ¹ and Prineha Narang ^{4,*}

¹*Aliro Technologies, Inc., Boston, Massachusetts 02135, USA*

²*John A. Paulson School of Engineering and Applied Sciences, Harvard University, Cambridge, Massachusetts 02138, USA*

³*Department of Electrical Engineering and Computer Science,*

Massachusetts Institute of Technology, Cambridge, Massachusetts 02139, USA

⁴*College of Letters and Science, University of California, Los Angeles (UCLA), California 90095, USA*



(Received 26 April 2022; revised 10 April 2023; accepted 7 June 2023; published 8 September 2023)

We present an approach to entanglement purification on complex quantum network architectures, that is, how a quantum network built from repeaters with limited processing fidelity can purify and distribute entanglement between users. In particular, we explore how noisy gates, depolarizing channels, and finite memory storage time influence the performance of entanglement purification in a quantum network. Finally, we apply the purification techniques we developed in the context of entanglement routing for different quantum network topologies in an effort to inform future design choices for quantum network configurations.

DOI: [10.1103/PhysRevResearch.5.033171](https://doi.org/10.1103/PhysRevResearch.5.033171)

I. INTRODUCTION

A quantum network (QN) [1–4] is used to generate, distribute, and process quantum information for a variety of applications. For many use cases, the most important prerequisite is entanglement shared between distant nodes, whether that is used for quantum computing [5–8], quantum cryptography [9], or quantum sensing [10,11]. Due to the inevitable photon loss along the transmission of quantum states, large-scale QNs are equipped with quantum repeaters [12–14]. Quantum repeaters are devices that are introduced in QNs in order to: (i) assist with entanglement routing [15–24] through entanglement swapping [25–27], (ii) enhance its quality through entanglement purification (also known as entanglement distillation) [28–32], and (iii) store it for synchronization purposes with quantum memories [33–36].

In this paper, we present the groundwork for a working QN built from repeaters with limited processing fidelity. In particular, we explore how network parameters influence the performance of entanglement purification, which in turn affects entanglement routing. The novel approach of this work is to introduce custom purification protocols for entanglement distribution in a QN, by taking into account noisy gates, lossy channels between quantum repeaters, and finite memory storage time. Note, that we evaluate our results with both perfect and imperfect gate fidelities in order to highlight the effect of gate imperfections across a network. We also contribute to the QN stack development [37–39] by demonstrating the performance of heuristic link costs for entanglement routing

protocols on a QN. Note that a QN stack has many different layers ranging from immediate point-to-point connectivity to routing of entanglement across the network [37].

The paper is structured as follows. In Sec. II we introduce several preliminary notions and terms of QNs. In Sec. III we review the concept of purification and introduce our optimized purification routine for a finite-memory repeater chain made up of channels with varied entanglement generation rates. We then discuss how this is connected to entanglement routing in Sec. IV, and we finally conclude this work in Sec. V.

II. QUANTUM NETWORK PRELIMINARIES

QNs can be characterized by three main components: (i) end nodes that refer to quantum processors that can receive and emit information, (ii) channels corresponding to classical and quantum communication links over long distances that connect the end nodes, and (iii) quantum repeaters, i.e., intermediate nodes along a communication line that act to manage photon loss across the network. Before we model the QN more rigorously, we introduce below the main components and methods of the physical entanglement distribution process.

A. Entanglement distribution

In our model the entangled pairs correspond to correlated qubits generated in the QN end nodes. Entangled quantum states are distributed among the end nodes through optical fibers that are modeled as quantum channels. The main characteristic of a quantum channel for communication purposes is photon loss, which is a function of the length over which the photon travels. Note that recent experiments have demonstrated successful long-range entanglement links, from terrestrial point-to-point links over a distance of 1000 km [40], to satellite-ground entanglement distribution [41,42].

An efficient way to distribute entanglement without direct transmission is through a process known as entanglement

*prineha@ucla.edu

Published by the American Physical Society under the terms of the Creative Commons Attribution 4.0 International license. Further distribution of this work must maintain attribution to the author(s) and the published article's title, journal citation, and DOI.

swapping [25–27]. While the fundamental method of producing an entangled pair is through emission from one source, two different entangled pairs can be connected into one by performing the appropriate measurement in one part of each state. In our case, this measurement is a joint measurement on the two qubits, and specifically a Bell-state measurement (BSM), meaning we project the qubits into one of the four entangled Bell states. This results in the entanglement of each of those qubit’s respective halves, leading to new entanglement between two qubits that have previously never interacted before. Swapping is a 1:1 relation, meaning that, for n, m pairs available for connection through a swapping procedure, only $\min(n, m)$ new pairs will be generated. Two-way communication is used to communicate successful swapping. For the purposes of this work, we assume that entanglement swapping occurs with unit probability, but with fidelity limited to gate operations [43].

Photon loss is the main limitation in the distribution of entanglement in long distances since the probability of successful transmission of a photon through a quantum channel decays exponentially with distance. In classical communication, this issue is tackled by introducing repeaters at various points along the channel to amplify the signal. However, due to the no-cloning theorem [44] this solution cannot be used in quantum communication schemes. A proposed method to overcome this problem is the use of quantum repeaters [12–14], which are devices that act as receivers and connectors of entangled pairs. They are introduced in the QN as intermediate nodes in order to help distribute the entanglement. They do so by performing entanglement swapping on the received quantum states and thus extend entanglement in further distances. Quantum repeaters are also equipped by protocols such as entanglement purification and error correction in order to mitigate the loss of photons during the channel transmission and the noise induced by other compartments such as quantum gates and measurement devices. For the purposes of this work, we consider repeaters that have the capability of performing one-qubit and two-qubit gate operations, conditioned on measurement outcomes. We also assume that the quantum repeaters have the resources and are capable of performing both purification and entanglement swapping [45]. Specifically, we consider purification protocols that are applied at most once per each entanglement swapping round. This process can be performed on multiple layers as long as it lasts no longer than the decoherence time. By allowing for flexibility in the stage at which purification occurs, we can perform the error detection at the point of largest impact. A schematic representation of a repeater is shown in Fig. 1.

Quantum repeaters rely on quantum memories [33–36] for storage of entangled pairs while purification and swapping processes are implemented. These memories have a buffer capable of storing a designated number of qubits for a given time. All necessary operations must be accomplished across all repeaters in the chain within the duration of the time in which the memory is coherent where t_{decoh} is the time at which the memory decoheres. We model the memory coherence time as a discrete time step, meaning that for $t < t_{\text{decoh}}$ the memory holds the received qubit with a static fidelity and for $t > t_{\text{decoh}}$ the qubit is lost. We assume that all memories are

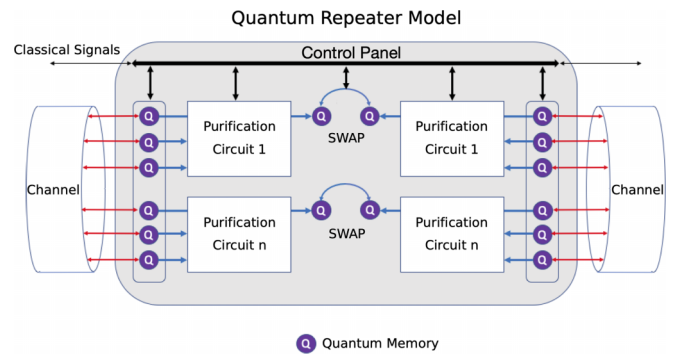


FIG. 1. A diagram representing the structure of a quantum repeater from our model. Stored qubits from adjacent channels are operated on by purification circuits, reducing the overall number of purified qubits to be swapped for generating long-range entanglement.

on-demand memories, i.e., they can retrieve and release the stored entangled pairs whenever required.

B. Quantum network

By arranging repeaters and their connecting channels in a distributed way, we can build a QN that offers multiple communication lines between end nodes [1–4]. Much like classical networks, we can imagine two users requesting to establish entanglement, and the network responding by assessing the network, determining the optimal chain of repeaters across which to distribute entanglement, and sending a signal to the physical layer to start the entanglement generation and swapping process. This network may monitor and decide the optimal path over which to route entanglement distribution, as well as the optimal method of distribution, i.e., implementing any purification processes needed to combat quantum state decoherence across the network.

It is worth discussing the current state of the art for hardware implementations of QNs. Superconducting circuits are a promising platform for implementing deterministic entanglement swapping and purification operations. Not only are these gate operations possible, but they have been experimentally implemented, producing Bell pairs with fidelities greater than 0.75 [46,47]. Single-qubit gate fidelities on superconducting circuits have exceeded 0.99 as early as 2014 [48], and controlled two-qubit gate fidelities have reached similarly high fidelities since 2016 [49]. The primary drawback of using superconducting qubits in QNs is the difficulty in microwave-to-optical transduction. The channels in QNs will most likely need to rely on photons for transportation of information, meaning quantum processors will need to convert these photons into whatever medium necessary for gate operation. However, current experimental implementations that match superconducting frequencies and bandwidths have only achieved total device efficiency on the level of 10^{-13} [50]. Proposals have been made to overcome this drawback through optically heralded entanglement of superconducting qubits [51] but experimental implementations are still in progress. Alternatives to superconducting qubits exist in the use of atomic ensembles, which have already been shown to have promising multiplexing capabilities [35,52,53]. However,

entanglement swapping and purification operations have yet to be demonstrated in this medium. Other promising platforms are the ones based on trapped ions [54] and nitrogen-vacancy centers [55]. Both of them are capable of relatively long qubit coherence time and the latter has already been used for an experimental implementation of a three-node network [55]. Note that reducing the need for any conversion processes, we could restrict our QN to an entirely linear-optics-based implementation. Entanglement swapping and teleportation have even been demonstrated in such a platform with Bell state fidelities on par with that shown in superconducting qubits [56]. However, due to the probabilistic nature of linear-optics gates, this method provides an extra obstacle in the scalability of a working QN, and so it is likely that medium conversion will be necessary, whether that be to superconducting qubits or some other medium capable of deterministic control.

To model a QN, we can consider a two-dimensional (2D) graph $G(V, E)$. Each node $v \in V$ is a repeater, with each edge $e \subseteq E$ representing a physical link acting as the communication channel between two repeater nodes. The network is synchronized to a clock where each time step is no longer than the memory decoherence time. E is characterized by its entanglement generation rate (EGR). Specifically, for each time step, $\text{EGR}_{i,j}$ is the number of entangled pairs generated between two nodes $v_i, v_j \subseteq V$, where each node possesses a half of the entangled state. We treat this generation as deterministic for this study, as we are specifically interested in how these varied rates affect expected distillable entanglement across a particular path.

Noise across the network, which is introduced mainly due to transmission channels, leads to imperfect (raw) Bell pairs, and thus each entanglement swap operation that concatenates single-hop segments results in a single segment of a lower fidelity than either of its two components. Note that fidelity for two arbitrary states ρ and σ is defined as $F = \text{tr}(\sqrt{\sqrt{\rho}\sigma\sqrt{\rho}})^2$ [57]. For the purposes of this work, we characterize any noise as complete depolarization. This is because the states that are produced can be written as mixing with isotropic noise, and hence forms the worst-case assumption of noise across a network. A pure Bell state $|\phi\rangle = \frac{1}{\sqrt{2}}(|00\rangle + |11\rangle)$ that mixes with isotropic noise can be written as a Werner state [58]

$$\rho = W|\phi\rangle\langle\phi| + \frac{1-W}{4}I_4, \quad (1)$$

where $W \in [0, 1]$.

The fidelity between the final state ρ and the pure Bell state $|\phi\rangle\langle\phi|$ is $F = \frac{3W+1}{4}$ [19]. These states are produced in the end nodes of the QN. Then, one half is sent through the link to its adjacent node while the other half is sent to the quantum memory. The quantum repeaters are placed in half the distance between two nodes, where each half is subsequently connected to another Werner state through a swapping procedure, either pre- or postpurification, resulting in a longer pair with an entanglement fidelity reflective of the chosen operations.

The output states of these operations are repeatedly brought back to a Werner state with identical fidelity using a series of random bilateral rotations. If we consider a chain of n neighboring Werner states that are connected in this method,

we find that the overall fidelity of the output state is [59]

$$F = \frac{1}{4} + \frac{3}{4} \left[\frac{p_2(4\eta^2 - 1)}{3} \right]^{n-1} \prod_{i=1}^n \frac{4F_i - 1}{3}, \quad (2)$$

where p_2 is the two-qubit gate fidelity associated with the probability of depolarization occurring during the gate operation (single-qubit gate fidelity p_1 are assumed to be equal to 1), and η is the measurement fidelity associated with the probability of a measurement reporting the incorrect result. In this paper, we compare perfect gate and measurement fidelities ($\eta = p_2 = 1$) and imperfect gate and measurement fidelities ($\eta = p_2 = 0.99$). No single-qubit errors are treated in this model as they are generally much lower. Given that we focus on a particular set of states, i.e., Werner states, entanglement can be characterized through the fidelity F between the actual state and the ideal Bell state, that we refer to as channel fidelity.

Figure 2 visualizes such a network as channels connecting neighboring repeaters that vary in the number of pairs generated in a single time step of the network. We define three different network parameter regimes where different routing strategies perform better. In near-perfect networks, we find that imperfect gate and channel fidelities may be small enough to enable a search for high-EGR (but potentially longer) paths. Low channel fidelity leads to accumulated decoherence that constrains the overall path length. By using more selective purification circuits on high-EGR channels, the network can increase the fidelity of individual channels in an effort to reduce decoherence across the network. For a network primarily limited by gate fidelity, purification is more advantageously performed post-BSM, and shorter paths with neighboring channels of near-identical entanglement generation rates will better sustain purification across these connected channels.

III. ENTANGLEMENT PURIFICATION

A. Introduction to entanglement purification

Purification protocols consist of performing local operations on n entangled pairs shared between two parties, resulting in a smaller number of higher-fidelity pairs. Typically, local operations consist of measurements, single-qubit gates, e.g., phase rotations, and two-qubit gates, e.g., CNOT gates, with different sequences depending on the specific protocol. Once all gate operations are complete, both parties perform a measurement and, depending on the outcome the resulting pair is determined to have a higher output fidelity, the entangled pair is stored or discarded. These protocols are probabilistic, leading to reduced rates from the initial entanglement generation rate of raw pairs. The resulting fidelity gain from a circuit is increased with the number of pairs sacrificed.

Purification protocols were discussed as early as 1996 by Bennett *et al.* in Ref. [60]. Briegel, Dür, Cirac, and Zoller developed methods of purification on a quantum repeater chain [59,61] in a nested fashion to detect errors introduced in the connection process. Entanglement pumping [59] and Bennett's recurrence protocol [28] provide a method for converting m pairs into a single pair of asymptotically high fidelity, limited only by the gate fidelity of the operators

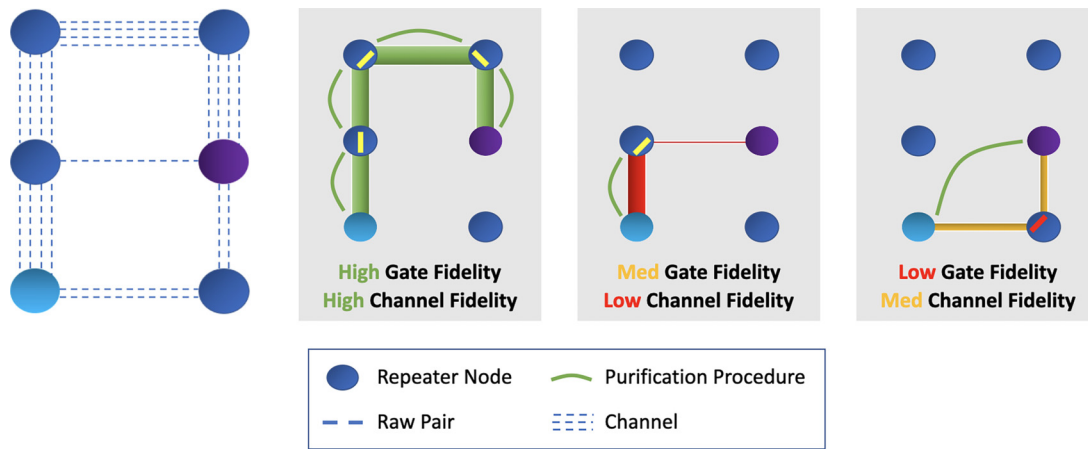


FIG. 2. (Left to right) The network over which we search for the best entanglement distribution procedure. Individual channels between neighboring nodes are made up of one or more raw entangled pairs. Under high gate and channel fidelities, routing can opt for longer paths with higher minimum EGR. When limited by channel fidelity, shorter paths become more attractive, and channels with high EGR between neighboring nodes allow more selective purification. With gate fidelity as a limiting factor, purification is best performed across multiple hops, leading to need for neighboring channels with near-identical EGR.

[62]. Optimizing the use of these protocols across repeater chains results in a nontrivial problem as resource constraints, channel characteristics, and input state quality all affect the purification strategies [63]. While entanglement pumping and recurrence protocols allow one to achieve an asymptotically high state fidelity [28], repeated gate operations can result in marginal returns in the latter stages of purification. To improve upon these schemes, much work has gone into developing and optimizing new purification schemes using multiple pairs, applying error correcting codes to explore a wider range of circuit options [64]. Recently, work by Krastanov *et al.* [65] developed a method for optimizing purification circuits with respect to circuit width, gate, and input state fidelity, utilizing permutation schemes [66,67] to increase the conversion efficiency. It should also be noted that Zwerger *et al.* [68] demonstrated the advantage of measurement-based quantum repeaters, which utilize large fully connected graph states to achieve more robust purification. However, as multipartite entanglement is currently much more difficult to implement experimentally, here we only focus on gate-based repeaters.

In this work, we perform two nested layers of purification, with the first performed between neighboring nodes, and the second performed across a maximum of three entangled links that have been joined through entanglement swapping. This scheme is inspired by the work of Bratzik *et al.* [63], where the authors explored the optimization of purification schemes with respect to the secret key rate. It was shown that for high gate fidelities and low channel purification success, the optimal scheme only involves performing purification between neighboring nodes. We extend this scheme by allowing a second layer of purification to extend across a maximum of three joined links. From here on out, we will define circuits that sacrifice a greater fraction of raw pairs as more selective circuits.

B. Entanglement generation rate

Suppose we have a repeater chain of (v_1, v_2, \dots, v_n) , where all repeaters v_i, v_{i+1} are neighbors of each other and u_1 would like to share entangled pairs with u_n . First, all repeaters

generate entanglement with their neighbors/neighbor in parallel and store the entangled links in memory. An intermediate repeater v_i will perform either a swap or a purify-and-swap operation when repeaters v_{i-1} and v_{i+1} are ready. The overall entanglement generation rate (EGR) with this protocol is equal or smaller than the raw EGR of one link. The expected EGR, R_e , between nodes v_1 and v_n will be

$$R_e \leq \min\{\text{Pur}_{1,2}, \dots, \text{Pur}_{n-1,n}\}, \quad (3)$$

where $\text{Pur}_{i,j}$ represents the raw $\text{EGR}_{i,j}$ postpurification. Specifically, $\text{Pur} \leq p_{\text{succ}} \times [\text{EGR}/k]$, where k denotes the number of pairs used in a particular circuit, and p_{succ} denotes the probability of success for that purification circuit to return a state with a higher fidelity. If a swapping operation is performed with no purification, then $\text{Pur} = \text{EGR}$. By decreasing the selectivity of circuits on lower-EGR channels and increasing the selectivity of circuits on higher-EGR channels, we can strike a balance of optimized EGR while still maintaining a usable fidelity. In this case, we do not include the time of circuit operation in our rate calculation as we assume all operations are able to take place in one time step of our network.

C. Hashing rate

A primary goal in quantum networking is to ensure maximum channel fidelity between source and destination. In quantum communication, the raw number of established entangled pairs is not a proper quantifier since decoherence of each pair reduces the quality of entanglement, which must be mitigated through purification. In order to characterize entanglement distribution across the network with respect to both the quantity (pair number) and quality (decoherence) of the states, we choose to make use the hashing method, which utilizes local unitary operations and one-way communication. This method induces the hashing rate, D_H , derived by Bennett *et al.* [69], which represents the yield of n purified pairs (near-perfect states) the source and destination can distill from m shared impure pairs of fidelity F , i.e.,

$$D_H = 1 + F \log_2 F + (1 - F) \log_2 [(1 - F)/3]. \quad (4)$$

Specifically, we want to use this measure to characterize the amount of pure Bell pairs we are able to distill given the parameters of the network. To this end, we multiply D_H by the number of entangled pairs generated from end to end after our distribution process is complete, n . This gives us a rate of entanglement per time step. Finally, for comparison purposes, we normalize our measure by the average EGR between nodes of the network, i.e.,

$$D_H \rightarrow D_H \times \frac{n}{\text{average EGR}}. \quad (5)$$

In the rest of the paper, the term hashing rate will refer to Eq. (5). This way, we have a measure that is a function of both the fidelity and the average EGR that allows us to effectively compare different repeater chains and purification schemes. As far as practical applications, D_H is also related to the asymptotic distillable key rate in a six-state quantum key distribution protocol [70].

While both fidelity and entangled pair rate play a role in determining the overall hashing rate, these two parameters have an inverse relationship, as in order to increase the fidelity of one entangled pair, we must reduce the overall number of distilled pairs shared through purification. QN protocols focus on maintaining high-fidelity entanglement while not excessively reducing the EGR through overly selective purification schemes.

D. Circuit optimization

We model our decoherence across a chain of repeaters with purification performed both along single links, and along longer links that have been connected through entanglement swapping operations. To model purification performed after a subset of entangled links have been joined together through swapping operations, we first calculate the fidelity of the new long-range entangled state using Eq. (2). We then calculate the output fidelity of a purification operation. Finally, we use Eq. (2) again to model the fidelity across a chain of these new long-range entangled states. This operation is repeated for two nested layers. This chain of repeaters is generated using an EGR uniformly spread from 8–32 raw entangled pairs per channel per time step. We first build a family of circuits that span different node sizes and are optimized for varying gate fidelities. We then perform an exhaustive search to determine a purification and entanglement swap protocol that provides the highest hashing rate on the generated chain.

For our purification optimization procedure, we first assign all channels the most selective distillation circuit we consider in this work, where $k = 8$ pairs are converted into one single high-fidelity pair. We chose $k = 8$ as our maximum selectivity, as increasingly selective circuits did not provide significantly increased hashing rate for our explored network parameters and repeater chain lengths. We then perform a purification relaxation process where we decrease the circuit selectivity across the channel/s with the lowest pair number postpurification, $\text{Pur}_{i,j}$. Without relaxation, these channels essentially act as bottlenecks on the overall expected entanglement generation rate R_e [see Eq. (3)], as R_e is limited by the minimum channel EGR postpurification. By relaxing circuit selectivity across these channels, we increase the overall R_e

of the chain, but at a reduced final fidelity. This relaxation process is continued until we determine an upper bound on achievable hashing rate [see Eq. (5)].

We develop a library of purification circuits optimized with respect to gate and measurement fidelity using optimization software written by Krastanov *et al.* [65]. Our channel EGR parameter includes consideration of a memory buffer large enough to hold all entangled pairs generated in a single time step, thereby allowing us to consider the advantage of wide circuits used in near-perfect gate conditions. While many works [71] have studied purification using standard protocols such as BBPSSW [28] (named after Bennett, Brassard, Popescu, Schumacher, Smolin, and Wootters) and DEJMPS [29] (named after Deutsch, Ekert, Jozsa, Macchiavello, Popescu, and Sanpera), we customize our protocols using circuits that are optimized to our network parameters.

Note that in this work we consider both pre- and post-BSM purification. If purification is best performed post-BSM, we must determine the number of hops over which to perform the purification protocol. We need to time our resource-intensive purification protocol so as to achieve the maximum fidelity increase with minimal qubits sacrificed. We limit the distance across which purification can be performed to three hops in order to ensure all communication time fits within the time step of the network. Each permutation of potential purification channel lengths is fed into our optimization scheme, along with our pre-BSM chain. In this way, our optimization protocol returns information both on circuit type and circuit timing.

E. Optimized hashing rate

We consider at most one round of purification per hop. However, after each entanglement swapping operation a new layer of hops is effectively created. Figure 3 shows the longest number of initial-chain hops over which purification was performed for a uniform quantum repeater chain, where channels between nodes each produced 20 raw Bell pairs per time step for a repeater separation of six hops. We observe the number of hops increase as gate fidelity drops, representing the preference for purification to correct for accumulated errors, in order to generate the most drastic improvement in fidelity at minimum number of sacrificial pairs. Additional plots detailing the hashing rate achieved for various entanglement generation rates are included in Appendix A.

As we introduce nonuniform quantum repeater chains, where channels between nodes have differing entanglement generation rates, we use asymmetric purification protocols that outperform symmetric protocols on a repeater chain with edges of varied entanglement generation rates. Specifically, we allow for different purification circuits to act across different edges of a selected repeater chain rather than enforcing a uniform purification routine. Note also that we only consider isotropic noise in this model, rather than biased noise that we could target with more granularity in the goal of improving purification schemes. Even with these abstractions, however, we find that purification optimization across a repeater chain is nontrivial, and we aim here to provide a framework for optimizing information flow across a network using more comprehensive models.

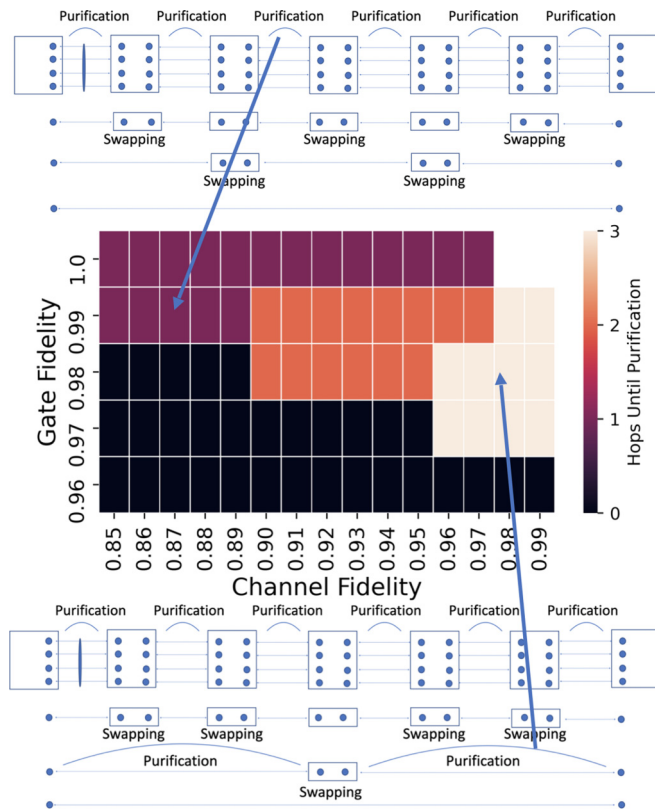


FIG. 3. Color map coded by maximal number of hops (of the initial chain) over which optimal purification was performed for varying gate and channel fidelity. 0's in the bottom left describe parameter settings where no distillable entanglement was achieved for any purification scheme explored. It should be noted that lower gate fidelity led to purification being optimally performed at higher levels of nesting, while higher gate fidelity means optimal purification protocol was performed only between neighboring nodes. Missing boxes mean no purification was needed to achieve optimal hashing rate. Diagrams above and below represent what the full swapping and purification scheme will be for the different numbers of hops. The repeater chain analyzed used a uniform channel EGR of 20 pairs/time step, and a path length of six hops.

IV. APPLICATION TO ENTANGLEMENT ROUTING

In a QN two nodes can be connected through multiple repeater chains. The selection of the optimal path is referred to as entanglement routing. In this section, we apply the purification techniques we developed in the previous section in the context of entanglement routing for different QN topologies.

A. Introduction to entanglement routing

The complicated problem of entanglement routing across a QN has been discussed in the literature before. Recently, Pirandola [15] bounded the ultimate limits for entanglement distribution and secret key generation in a chain of repeaters in a QN. Schoute *et al.* [16] developed routing protocols on specific network topologies and found scaling laws under the assumption that each link generates a perfect EPR pair in every time slot and each repeater's actions are limited to perfect BSM's. Pant *et al.* [17] developed local-knowledge

and global-knowledge QN routing protocols using a simplified model where the only source of imperfection is pure photon loss. Chakraborty *et al.* [18] used a similar pure photon loss model to test performance of adapted classical networking routing algorithms on a QN under the strain of multiple concurrent requests. Chakraborty *et al.* [19] constructed an efficient linear-programming formulation, where they approached entanglement routing using a multicommodity flow-based approach with perfect gate operations and imperfect channels without purification. Van Meter *et al.* [20] analyzed topologically complex networks and defined measures for quantifying total work along a path and informing path selection. Azuma and Kato [21] studied entanglement distribution in QNs based on quantum repeaters running in parallel. It is also worth mentioning that techniques that maximize the entanglement distribution rate in homogeneous repeater chains were proposed in Ref. [22], and techniques that minimize the entangled pair generation latency were proposed in Ref. [23]. Finally, the robustness of QNs with noisy quantum repeaters for various topologies was studied in Ref. [24].

B. Results

Since the hashing rate [see Eq. (5)] is a function of both EGR and fidelity, path selection cannot be reduced to a simple shortest-distance or max-flow problem. Different network parameter regimes may require different routing methods that maximize the hashing rate between two repeaters. However, to compare all possible paths across a network while customizing a purification routine for each one becomes an exponentially difficult problem. By developing an appropriate cost function to select for paths that have a greater overall EGR, we open up the possibility of using Dijkstra's weighted algorithm [72] to reduce the search time to find a decent path. It is not at all obvious whether a weighted path algorithm has a place in optimizing such a complex problem, particularly since that approach requires the overall cost function used to be a summation of individual edge costs, which does not match the functional form of the hashing rate [Eq. (4)]. The fact that it is not clear if a Dijkstra's weighted algorithm can be used for entanglement routing was discussed in Ref. [73], where an alternative way to solve this problem was proposed. See also Ref. [74] where the authors propose another way to deal with this problem.

To gain insight on constructive useful heuristics for path selection, we first perform a search over all possible paths between two end nodes on a network with a cutoff length of ten hops. This means that even if the shortest distance between two end nodes is less than ten hops away, we consider all paths available in the network, subject to our cutoff length. By allowing for longer candidate paths, we can explore the trade-off between the additional decoherence caused by a longer repeater chain and the potentially increased minimum EGR that may be available since we are not restricting ourselves to only the shortest paths. The cutoff length was selected to reduce computational time. The longest distance we consider between two end nodes is eight hops.

With our method from the previous section, we can find a path with maximal hashing rate between source to destination

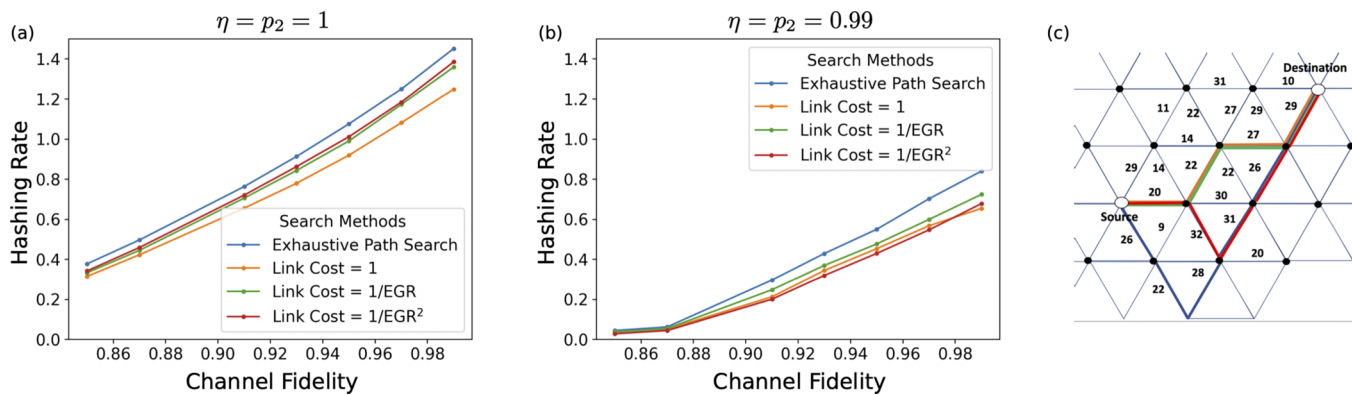


FIG. 4. A comparison of the hashing rate (normalized by average channel EGR) achieved using an exhaustive path search vs. Dijkstra’s weighted algorithm with three different link costs. A link cost of $1/\text{EGR}$ and $1/\text{EGR}^2$ lead to comparable performances with an exhaustive path search. (a) corresponds to $\eta = p_2 = 1$ and (b) to $\eta = p_2 = 0.99$. Simulations were performed on a triangular lattice with an end node separation of four hops. EGR was uniformly spread from 8–32 raw entangled pairs per channel per timestep. An example of four different paths in a triangular lattice is presented in (c) for $\eta = p_2 = 1$ and $F = 0.99$. Numbers listed by edges detail channel EGR. Path found by exhaustive path search implies a search for maximal minimum EGR along a path, while still balancing path length constraints.

on a network. By using a Dijkstra’s weighted algorithm with an appropriate link cost, we can converge to a solution without needing to examine all possible paths. To determine an appropriate cost function for our channels, we compared three different channel costs. We used a link cost of 1 to signify a search for the shortest path from source to destination. We compared this to a link cost of $1/\text{EGR}$, and a link cost of $1/\text{EGR}^2$. Both of these latter functions will weight (with different degrees) towards channels that have much higher entanglement generation rates. While entanglement generation rate certainly has a logical place in the cost function of a link, it is not obvious what functional form that cost should be in. In this case, $1/\text{EGR}^2$ will opt towards longer, higher throughput paths, while $1/\text{EGR}$ may punish length a bit more while still preferring higher throughput paths than a link cost of 1.

Figures 4(a) and 4(b) plot the hashing rate achieved with paths found using a Dijkstra’s weighted algorithm with appropriate link costs, as well as the hashing rate achieved using paths found by a time-intensive exhaustive path search. In the limit of perfect gate and channel fidelities, we find that Dijkstra’s weighted algorithm with a link cost of $1/\text{EGR}^2$ will slightly outperform a link cost of $1/\text{EGR}$, while the inverse is true for lower fidelities across the network. A cost of $1/\text{EGR}^2$ is more selective for higher channel EGRs to the point where longer paths become more attractive if they allow for increased overall flow (such as when states and operations have near-perfect fidelity). A cost of $1/\text{EGR}$ is less selective towards higher channel EGRs and, comparatively, more selective toward shorter path lengths. However, we find that, in the limit of low gate and channel fidelities, there is little difference between the performance of our exhaustive path search and a weighted algorithm with a link cost of $1/\text{EGR}$ or $1/\text{EGR}^2$. For all network parameters, a link cost of 1 did not outperform any of the costs that consider entanglement generation.

Our work shows that the hashing rate achieved in a path found using Dijkstra’s weighted algorithm comes very close to that found using our exhaustive path search, particularly if an effective link cost is utilized. Note that for the Dijkstra’s algorithm the purification protocol is not taken into account

because the Dijkstra’s algorithm is based on the unnormalized Hashing bound that does not depend on the EGR, but for the exhaustive path search the purification protocol is taken into account since in that case the normalized Hashing bound was used. We also see that the inclusion of imperfect gate fidelities in our calculations results in significantly reducing our rates across the network from those achieved in Fig. 4(a) where the gate fidelity equals 1, to Fig. 4(b) where the gate fidelity equals 0.99, motivating the need to account for processor imperfections in QN models. Figure 4(c) depicts a sample of paths chosen using the three different path search methods for a network of perfect gate and measurement fidelities, and channel fidelities of 0.99. Note that our weighted algorithms did not include component fidelities as link cost inputs. Similar comparisons for path searches on a square lattice network and a hexagonal lattice network are displayed in Appendix B.

V. DISCUSSION AND CONCLUSIONS

In this work we analyzed entanglement purification protocols for distributing entanglement among source-destination pairs. We extensively discussed our treatment of entanglement purification routines to be performed on repeater chains of varied entanglement generation across links with limited memory decoherence time. This was followed by an application of those purification methods to different routing schemes, and a discussion of appropriate link costs for Dijkstra’s weighted path algorithm. The approach and calculations presented here provide a baseline for entanglement distribution on near-term QNs with resource and performance constraints on individual repeaters, as well as the consideration of varied entanglement purification schemes optimized for channel bandwidth and repeater gate operation fidelity. We have used the hashing rate in order to characterize the performance of the QN.

QNs are critical components for the development of large-scale quantum systems. Emerging quantum applications will drive new requirements on the underlying QN devices and protocols and fundamental to these future QNs

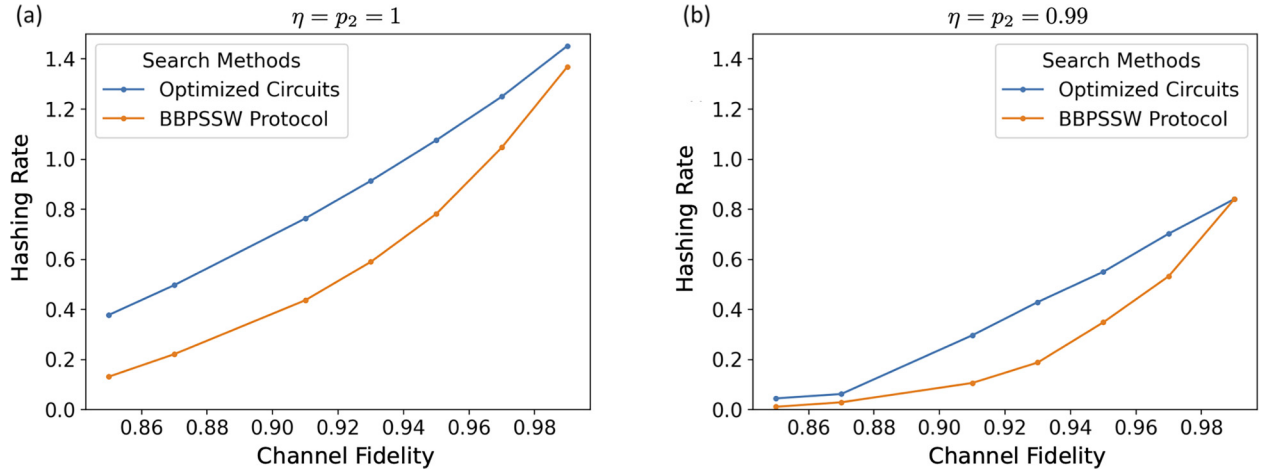


FIG. 5. A comparison of the hashing rate (normalized by average channel EGR) achieved using circuits from our circuit optimization routine vs. a standard BBPSSW protocol for a path length distance of four hops. EGR spread from 8–32 raw entangled pairs per channel per timestep on a triangular topology. (a) corresponds to $\eta = p_2 = 1$ and (b) to $\eta = p_2 = 0.99$.

is entanglement routing. Looking ahead, the development of constraint-based entanglement routing protocols based on topology, noise models, link costs, resource usage, and diverse quantum repeater architectures will be crucial in overcoming the limitations of near-term QNs. This work opens up a number of new questions for future exploration, e.g., the development of path selection heuristics that take entanglement purification into account. Even in a simplified model where entanglement generation is deterministic and coherence time is finite, we demonstrate the need to tune purification protocols across different channels of the network in order to distribute information at the highest rate. Accounting for dynamic noise models will allow us to better optimize entanglement purification and memory storage time for a synchronized network continuously generating entanglement. In addition, by decomposing our entanglement generation rate into probabilistic source rates and sizing of qubit buffers on individual repeaters, we will be able to explore optimal architectures for repeaters given the network topology and overall figures of merit.

ACKNOWLEDGMENTS

The authors thank Profs. D. Towsley (University of Massachusetts), S. Guha (University of Arizona), and Dr. M. Fanto (AFRL) for insightful discussions and comments on the work. M.V. is partially supported by the US Air Force under FA8750-20-P-1721. S.T. is supported by the NSF Engineering Research Center (ERC) Center for Quantum Networks and NSF RAISE-QAC-QSA, Grant No. DMR2037783. S.K. is partially supported under the US Department of Energy, Office of Science, Basic Energy Sciences (BES), Materials Sciences and Engineering Division under FWP ERKCK47. P.N. acknowledges support as a Moore Inventor Fellow through Grant No. GBMF8048 and gratefully acknowledges support from the Gordon and Betty Moore Foundation as well as support from a NSF CAREER Award under Grant No. NSF-ECCS-1944085. Simulations made use of the NETWORKX program for analyzing networks in PYTHON [75].

APPENDIX A: CIRCUIT OPTIMIZATION

The software used to design the circuits in our purification routines employs a generic algorithm to optimize for either a weighted average of fidelity and success probability, or the hashing rate. Inputs to the algorithm include the number of sacrificial pairs, gate operation errors, measurement operation errors, and the fidelity of the entangled pairs. In order to produce the library of circuits used for our purification routines, we created an optimized purification circuit for each of n sacrificial pairs, where n is a number from 1–10. A purification circuit was created for each gate fidelity explored in our paper. State fidelity was always held at 0.9 as we found that variance in the input state fidelity did not have a large affect on the optimal circuit used. The optimization measure was set to maximize the fidelity of the target pair.

This library of circuits was then fed into a purification optimization routine for the results shown in the paper. This purification optimization routine operates on a candidate path by first generating a list of single-hop purification circuit combinations, meaning the possible pairs of nodes that entanglement purification can be performed. This list is generated through a similar process as used in our purification relaxation routine, however, instead of only retaining the combination with the highest hashing rate, we keep a list of all combinations explored as these will be fed into higher nested layers. Given the possible purification combinations within a given layer of nodes, we can create a list that includes all possible purification combinations among the different layers, that we refer to as purification permutations. This routine uses our purification relaxation process to determine the highest hashing rate achievable for each permutation. Finally, our function returns the highest hashing rate achieved over all permutations. Physically, this tells us at what point purification was optimally performed and with which circuits.

In Fig. 5 we compare our purification routine to that of the BBPSSW protocol [28]. Specifically, we replace circuits used from our circuit optimization routine with recurrent purification using the single-selection circuit for n rounds where $n \in [1, \dots, 4]$. We can see that our customized routine

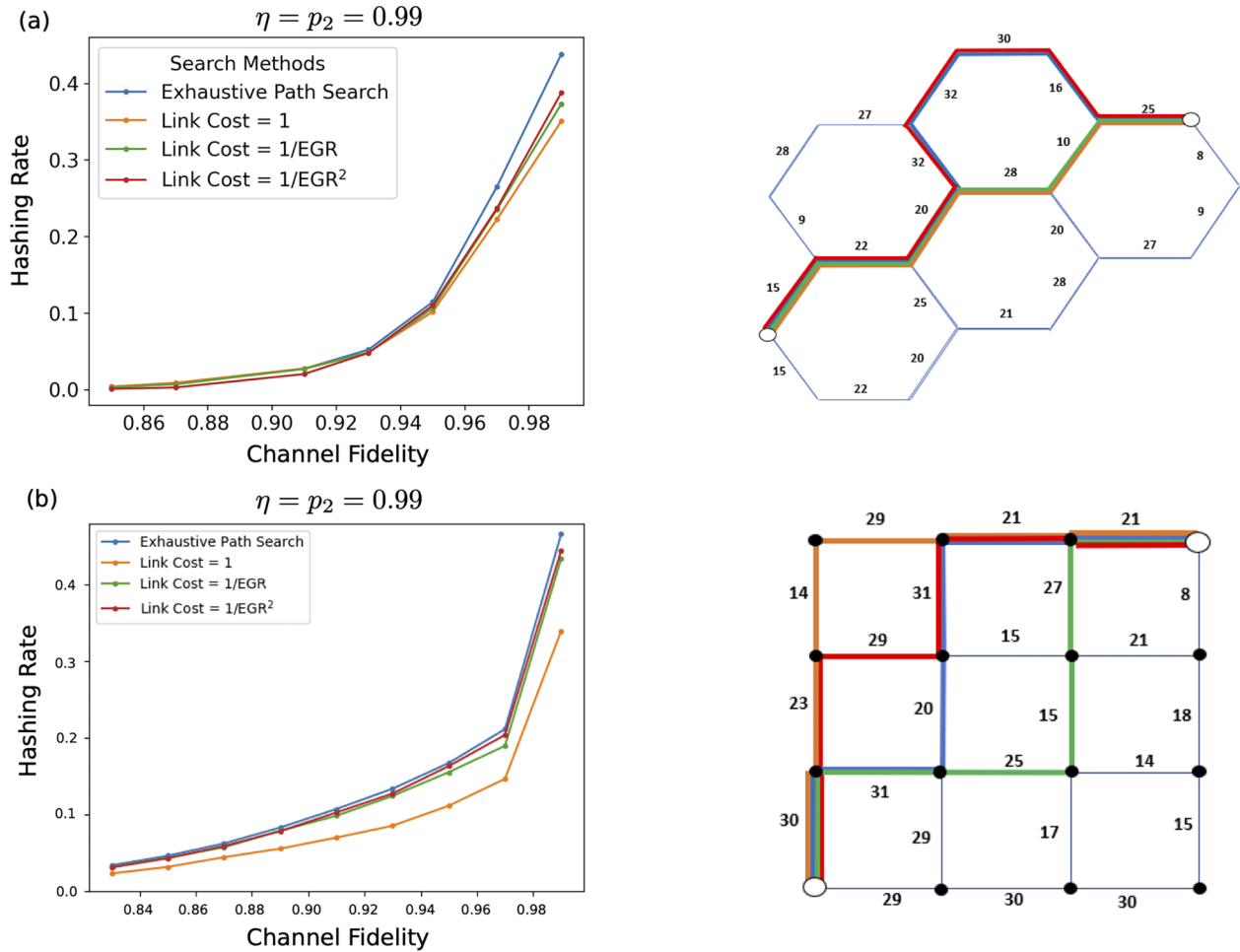


FIG. 6. On the left-hand side panels there is a comparison of the hashing rate (normalized by average channel EGR) achieved using an exhaustive path search vs. Dijkstra’s weighted algorithm for a path length distance of six hops and $\eta = p_2 = 0.99$. EGR spread from 8–32 raw entangled pairs per channel per time step on a hexagonal topology (a) and a square topology (b). On the right-hand side panels sample paths are found on an hexagonal and a square lattice, respectively, for $\eta = p_2 = 1$ and $F = 0.99$ and with a random uniform EGR spread of 8–32. Optimal path found in blue, shortest path found in orange, Dijkstra’s weighted algorithm with link cost of $1/EGR$ (green), Dijkstra’s weighted algorithm with link cost of $1/EGR^2$ (red).

outperforms the BBPSSW protocol in terms achievable hashing rate. It is worth noting that the BBPSSW protocol is capable of operation using fewer memories (technically we only need two memories for each recurrence). Regardless, we can think of the BBPSSW protocol as a lower bound on what our optimized circuits can achieve in the limit of low memory buffer on our repeaters.

APPENDIX B: ENTANGLEMENT ROUTING IN DIFFERENT TOPOLOGIES

Figure 6 compares the hashing rate found from our exhaustive path search to that found using a Dijkstra’s weighted

algorithm with appropriate cost functions for a hexagonal and a square lattice. Here, we kept the y axis the same between both graphs to highlight the decrease introduced by imperfect gate fidelities. In the case of perfect gate fidelities, we see the $1/EGR^2$ cost function performs higher for both topologies, as longer paths have a smaller impact on the overall fidelity degradation.

Figure 6 shows also a sample of paths found on varying network topologies. We see that appropriately weighted cost functions perform well in a variety of different network structures. As in the main text, we select our gate fidelity to 1 and our channel fidelity to 0.99, to highlight instances where the best path may not be the shortest path between points.

[1] R. Van Meter, *Quantum Networking* (John Wiley & Sons, New York, 2014)
 [2] H. J. Kimble, The quantum internet, *Nature (London)* **453**, 1023 (2008).
 [3] D. Castelvecchi, The quantum internet has arrived (and it hasn’t), *Nature (London)* **554**, 289 (2018).

[4] S. Wehner, D. Elkouss, and R. Hanson, Quantum internet: A vision for the road ahead, *Science* **362**, eaam9288 (2018).
 [5] A. Broadbent and C. Schaffner, Quantum cryptography beyond quantum key distribution, *Des. Codes Cryptogr.* **78**, 351 (2016).

- [6] R. Beals, S. Brierley, O. Gray, A. W. Harrow, S. Kutin, N. Linden, D. Shepherd, and M. Stather, Efficient distributed quantum computing, *Proc. R. Soc. A* **469**, 20120686 (2013).
- [7] W. Ge, K. Jacobs, Z. Eldredge, A. V. Gorshkov, and M. Foss-Feig, Distributed Quantum Metrology with Linear Networks and Separable Inputs, *Phys. Rev. Lett.* **121**, 043604 (2018).
- [8] J. F. Fitzsimons, Private quantum computing: an introduction to blind quantum computing and related protocols, *npj Quantum Inf.* **3**, 23 (2017).
- [9] C. H. Bennett and G. Brassard, Quantum cryptography: Public key distribution and coin tossing, *Theor. Comput. Sci.* **560**, 7 (2014).
- [10] Z. Eldredge, M. Foss-Feig, J. A. Gross, S. L. Rolston, and A. V. Gorshkov, Optimal and secure measurement protocols for quantum sensor networks, *Phys. Rev. A* **97**, 042337 (2018).
- [11] T. J. Proctor, P. A. Knott, and J. A. Dunningham, Multiparameter Estimation in Networked Quantum Sensors, *Phys. Rev. Lett.* **120**, 080501 (2018).
- [12] N. Sangouard, C. Simon, H. de Riedmatten, and N. Gisin, Quantum repeaters based on atomic ensembles and linear optics, *Rev. Mod. Phys.* **83**, 33 (2011).
- [13] C. Jones, D. Kim, M. T. Rakher, P. G. Kwiat, and T. Ladd, Design and analysis of communication protocols for quantum repeater networks, *New J. Phys.* **18**, 083015 (2016).
- [14] M. Pant, H. Krovi, D. Englund, and S. Guha, Rate-distance tradeoff and resource costs for all-optical quantum repeaters, *Phys. Rev. A* **95**, 012304 (2017).
- [15] S. Pirandola, End-to-end capacities of a quantum communication network, *Commun. Phys.* **2**, 51 (2019).
- [16] E. Schoute, L. Mancinska, T. Islam, I. Kerenidis, and S. Wehner, Shortcuts to quantum network routing, [arXiv:1610.05238](https://arxiv.org/abs/1610.05238).
- [17] M. Pant, H. Krovi, D. Towsley, L. Tassiulas, L. Jiang, P. Basu, D. Englund, and S. Guha, Routing entanglement in the quantum internet, *npj Quantum Inf.* **5**, 25 (2019).
- [18] K. Chakraborty, F. Rozpedek, A. Dahlberg, and S. Wehner, Distributed routing in a quantum internet, [arXiv:1907.11630](https://arxiv.org/abs/1907.11630).
- [19] K. Chakraborty, D. Elkouss, B. Rijsman, and S. Wehner, Entanglement distribution in a quantum network: A multicommodity flow-based approach, *IEEE Trans. Quantum Eng.* **1**, 4101321 (2020).
- [20] R. Van Meter, T. Satoh, T. D. Ladd, W. J. Munro, and K. Nemoto, Path selection for quantum repeater networks, *Netw. Sci.* **3**, 82 (2013).
- [21] K. Azuma and G. Kato, Aggregating quantum repeaters for the quantum internet, *Phys. Rev. A* **96**, 032332 (2017).
- [22] W. Dai, T. Peng, and M. Z. Win, Optimal remote entanglement distribution, *IEEE J. Sel. Areas Commun.* **38**, 540 (2020).
- [23] M. Ghaderibaneh, C. Zhan, H. Gupta, and C. R. Ramakrishnan, Efficient quantum network communication using optimized entanglement swapping trees, *IEEE Trans. Quantum Eng.* **3**, 4100420 (2022).
- [24] B. C. Coutinho, W. J. Munro, K. Nemoto, and Y. Omar, Robustness of noisy quantum networks, *Commun. Phys.* **5**, 105 (2022).
- [25] C. H. Bennett, G. Brassard, C. Crépeau, R. Jozsa, A. Peres, and W. K. Wootters, Teleporting an unknown quantum state via dual classical and Einstein-Podolsky-Rosen channels, *Phys. Rev. Lett.* **70**, 1895 (1993).
- [26] M. Żukowski, A. Zeilinger, M. A. Horne, and A. K. Ekert, “Event-ready-detectors” Bell Experiment Via Entanglement Swapping, *Phys. Rev. Lett.* **71**, 4287 (1993).
- [27] A. M. Goebel, C. Wagenknecht, Q. Zhang, Y.-A. Chen, K. Chen, J. Schmiedmayer, and J.-W. Pan, Multistage Entanglement Swapping, *Phys. Rev. Lett.* **101**, 080403 (2008).
- [28] C. H. Bennett, G. Brassard, S. Popescu, B. Schumacher, J. A. Smolin, and W. K. Wootters, Purification of Noisy Entanglement and Faithful Teleportation via Noisy Channels, *Phys. Rev. Lett.* **76**, 722 (1996).
- [29] D. Deutsch, A. Ekert, R. Jozsa, C. Macchiavello, S. Popescu, and A. Sanpera, Quantum Privacy Amplification and the Security of Quantum Cryptography over Noisy Channels, *Phys. Rev. Lett.* **77**, 2818 (1996).
- [30] F. Rozpedek, T. Schiet, L. P. Thinh, D. Elkouss, A. C. Doherty, and S. Wehner, Optimizing practical entanglement distillation, *Phys. Rev. A* **97**, 062333 (2018).
- [31] X. Zhao, B. Zhao, Z. Wang, Z. Song, and X. Wang, Practical distributed quantum information processing with LOCCNet, *Npj Quantum Inf.* **7**, 159 (2021).
- [32] S. Jansen, K. Goodenough, S. de Bone, D. Gijswijt, and D. Elkouss, Enumerating all bilocal clifford distillation protocols through symmetry reduction, *Quantum* **6**, 715 (2022).
- [33] R. Zhao, Y. O. Dudin, S. D. Jenkins, C. J. Campbell, D. N. Matsukevich, T. A. B. Kennedy, and A. Kuzmich, Long-lived quantum memory, *Nature Phys.* **5**, 100 (2009).
- [34] M. Reagor, W. Pfaff, C. Axline, R. W. Heeres, N. Ofek, K. Sliwa, E. Holland, C. Wang, J. Blumoff, K. Chou, M. J. Hatridge, L. Frunzio, M. H. Devoret, L. Jiang, and R. J. Schoelkopf, Quantum memory with millisecond coherence in circuit qed, *Phys. Rev. B* **94**, 014506 (2016).
- [35] F. Bussi eres, N. Sangouard, M. Afzelius, H. Riedmatten, C. Simon, and W. Tittel, Prospective applications of optical quantum memories, *J. Mod. Opt.* **60**, 1519 (2013).
- [36] Z. Xu, Y. Wu, L. Tian, L. Chen, Z. Zhang, Z. Yan, S. Li, H. Wang, C. Xie, and K. Peng, Long Lifetime and High-Fidelity Quantum Memory of Photonic Polarization Qubit by Lifting Zeeman Degeneracy, *Phys. Rev. Lett.* **111**, 240503 (2013).
- [37] A. Pirker and D ur, A quantum network stack and protocols for reliable entanglement-based networks, *New J. Phys.* **21**, 033003 (2019).
- [38] R. Van Meter, T. D. Ladd, W. J. Munro, and K. Nemoto, System design for a long-line quantum repeater, *IEEE/ACM Trans. Networking* **17**, 1002 (2009).
- [39] A. Dahlberg, M. Skrzypczyk, T. Coopmans, L. Wubben, F. Rozpedek, M. Pompili, A. Stolk, P. Pawelczak, R. Knegjens, J. de Oliveira Filho, R. Hanson, and S. Wehner, A link layer protocol for quantum networks, in *Proceedings of the ACM Special Interest Group on Data Communication* (ACM, New York, 2019).
- [40] J. Yin, Y.-H. Li, S.-K. Liao, M. Yang, Y. Cao, L. Zhang, J.-G. Ren, W.-Q. Cai, W.-Y. Liu, and J.-W. Pan, Entanglement-based secure quantum cryptography over 1,120 kilometres, *Nature (London)* **582**, 501 (2020).
- [41] J. Yin, Y. Cao, Y.-H. Li, S.-K. Liao, L. Zhang, J.-G. Ren, W.-Q. Cai, W.-Y. Liu, B. Li, and J.-W. Pan, Satellite-based entanglement distribution over 1200 kilometers, *Science* **356**, 1140 (2017).
- [42] J.-G. Ren, P. Xu, H.-L. Yong, L. Zhang, S.-K. Liao, J. Yin, W.-Y. Liu, W.-Q. Cai, M. Yang, and J.-W. Pan, Ground-to-satellite quantum teleportation, *Nature (London)* **549**, 70 (2017).

- [43] P. Krantz, M. Kjaergaard, F. Yan, T. P. Orlando, S. Gustavsson, and W. D. Oliver, A quantum engineer's guide to superconducting qubits, *Appl. Phys. Rev.* **6**, 021318 (2019).
- [44] W. K. Wootters and W. H. Zurek, A single quantum cannot be cloned, *Nature (London)* **299**, 802 (1982).
- [45] S. Muralidharan, L. Li, J. Kim, N. Lütkenhaus, M. D. Lukin, and L. Jiang, Optimal architectures for long distance quantum communication, *Sci. Rep.* **6**, 20463 (2016).
- [46] W. Ning, X.-J. Huang, P.-R. Han, H. Li, H. Deng, Z.-B. Yang, Z.-R. Zhong, Y. Xia, K. Xu, D. Zheng, and S.-B. Zheng, Deterministic Entanglement Swapping in a Superconducting Circuit, *Phys. Rev. Lett.* **123**, 060502 (2019).
- [47] B. K. Behera, S. Seth, A. Das, and P. K. Panigrahi, Demonstration of entanglement purification and swapping protocol to design quantum repeater in IBM quantum computer, *Quant. Info. Proc.* **18**, 108 (2019).
- [48] R. Barends, J. Kelly, A. Megrant, A. Veitia, D. Sank, E. Jeffrey, T. C. White, J. Mutus, A. G. Fowler, B. Campbell, Y. Chen, Z. Chen, B. Chiaro, A. Dunsworth, C. Neill, P. O'Malley, P. Roushan, A. Vainsencher, J. Wenner, A. N. Korotkov *et al.*, Superconducting quantum circuits at the surface code threshold for fault tolerance, *Nature (London)* **508**, 500 (2014).
- [49] S. Sheldon, E. Magesan, J. M. Chow, and J. M. Gambetta, Procedure for systematically tuning up cross-talk in the cross-resonance gate, *Phys. Rev. A* **93**, 060302(R) (2016).
- [50] J. G. Bartholomew, J. Rochman, T. Xie, M. J. Kindem, A. Ruskuc, I. Craiciu, M. Lei, and A. Faraon, On-chip coherent microwave-to-optical transduction mediated by ytterbium in yvo4, *Nature Commun.* **11**, 3266 (2020).
- [51] S. Krastanov, H. Raniwala, J. Holzgrafe, K. Jacobs, M. Lončar, M. J. Reagor, and D. R. Englund, Optically Heralded Entanglement of Superconducting Systems in Quantum Networks, *Phys. Rev. Lett.* **127**, 040503 (2021).
- [52] W. Chang, C. Li, Y.-K. Wu, N. Jiang, S. Zhang, Y.-F. Pu, X.-Y. Chang, and L.-M. Duan, Long-Distance Entanglement between a Multiplexed Quantum Memory and a Telecom Photon, *Phys. Rev. X* **9**, 041033 (2019).
- [53] N. Sinclair, E. Saglamyurek, H. Mallahzadeh, J. A. Slater, M. George, R. Ricken, M. P. Hedges, D. Oblak, C. Simon, W. Sohler, and W. Tittel, Spectral Multiplexing for Scalable Quantum Photonics using an Atomic Frequency Comb Quantum Memory and Feed-Forward Control, *Phys. Rev. Lett.* **113**, 053603 (2014).
- [54] R. Reichle, D. Leibfried, E. Knill, J. Britton, R. B. Blakestad, J. D. Jost, C. Langer, R. Ozeri, S. Seidelin, and D. J. Wineland, Experimental purification of two-atom entanglement, *New J. Phys.* **443**, 838 (2006).
- [55] N. Kalb, A. A. Reiserer, P. C. Humphreys, J. J. W. Bakermans, S. J. Kamerling, N. H. Nickerson, S. C. Benjamin, D. J. Twitchen, M. Markham, and R. Hanson, Entanglement distillation between solid-state quantum network nodes, *Science* **356**, 928 (2017).
- [56] C. Schmid, N. Kiesel, U. Weber, R. Ursin, A. Zeilinger, and H. Weinfurter, Quantum teleportation and entanglement swapping with linear optics logic gates, *New J. Phys.* **11**, 033008 (2009).
- [57] R. Jozsa, Fidelity for mixed quantum states, *J. Mod. Opt.* **41**, 2315 (1994).
- [58] R. F. Werner, Quantum states with einstein-podolsky-rosen correlations admitting a hidden-variable model, *Phys. Rev. A* **40**, 4277 (1989).
- [59] W. Dür, H.-J. Briegel, J. I. Cirac, and P. Zoller, Quantum repeaters based on entanglement purification, *Phys. Rev. A* **59**, 169 (1999).
- [60] C. H. Bennett, H. J. Bernstein, S. Popescu, and B. Schumacher, Concentrating partial entanglement by local operations, *Phys. Rev. A* **53**, 2046 (1996).
- [61] H.-J. Briegel, W. Dür, J. I. Cirac, and P. Zoller, Quantum Repeaters: The Role of Imperfect Local Operations in Quantum Communication, *Phys. Rev. Lett.* **81**, 5932 (1998).
- [62] K. Fujii and K. Yamamoto, Entanglement purification with double selection, *Phys. Rev. A* **80**, 042308 (2009).
- [63] S. Bratzik, S. Abruzzo, H. Kampermann, and D. Bruß, Quantum repeaters and quantum key distribution: The impact of entanglement distillation on the secret key rate, *Phys. Rev. A* **87**, 062335 (2013).
- [64] H. Aschauer, Quantum communication in noisy environments, Ph.D. thesis, LMU München, 2005.
- [65] S. Krastanov, V. V. Albert, and L. Jiang, Optimized entanglement purification, *Quantum* **3**, 123 (2019).
- [66] J. Dehaene, M. Van den Nest, B. De Moor, and F. Verstraete, Local permutations of products of bell states and entanglement distillation, *Phys. Rev. A* **67**, 022310 (2003).
- [67] H. Bombin and M. A. Martin-Delgado, Entanglement distillation protocols and number theory, *Phys. Rev. A* **72**, 032313 (2005).
- [68] M. Zwerger, W. Dür, and H. J. Briegel, Measurement-based quantum repeaters, *Phys. Rev. A* **85**, 062326 (2012).
- [69] C. H. Bennett, D. P. DiVincenzo, J. A. Smolin, and W. K. Wootters, Mixed-state entanglement and quantum error correction, *Phys. Rev. A* **54**, 3824 (1996).
- [70] G. Murta, F. Rozpedek, J. Ribeiro, D. Elkouss, and S. Wehner, Key rates for quantum key distribution protocols with asymmetric noise, *Phys. Rev. A* **101**, 062321 (2020).
- [71] W. Dür and H. J. Briegel, Entanglement purification and quantum error correction, *Rep. Prog. Phys.* **70**, 1381 (2007).
- [72] E. W. Dijkstra, A note on two problems in connexion with graphs, *Numer. Math.* **1**, 269 (1959).
- [73] M. Caleffi, Optimal routing for quantum networks, *IEEE Access* **5**, 22299 (2017).
- [74] L. Bugalho, B. C. Coutinho, F. A. Monteiro, and Y. Omar, Distributing multipartite entanglement over noisy quantum networks, *Quantum* **7**, 920 (2023).
- [75] A. A. Hagberg, D. A. Schult, and P. J. Swart, Exploring network structure, dynamics, and function using networkx, in *Proceedings of the 7th Python in Science Conference (SciPy 2008)*, edited by G. Varoquaux, T. Vaught, and J. Millman (2008), pp. 11–15.